INNOVATIONS IN MOLECULAR BIOTECHNOLOGY
2023, VOL. 1, ISSUE 1, pp. 1-6
https://doi.org/10.61577/imb.2023.100005

RESEAPRO JOURNALS

ORIGINAL ARTICLE

OPEN ACCESS

The study of RYR1 expression profile in rabbit muscle tissues

Kiranbala Jena and Lipsha Ray

Department of Biotechnology, Utkal University, Bhubaneswar, Odisha, India

ABSTRACT

Calcium ion (Ca^{2+}) cycling within the sarcoplasmic reticulum (SR) is a tightly controlled process that involves the coordinated actions of ryanodine receptors (RyRs), which mediate calcium release, and sarco/endoplasmic reticulum Ca^{2+}-ATPase (SERCA) pumps, which facilitate calcium reuptake. In skeletal muscle, RyR1 serves as a key calcium release channel, playing a central role in excitation–contraction (EC) coupling-the mechanism by which an electrical signal at the muscle membrane leads to muscle contraction. Among the muscles examined, the tibialis anterior (TA)-the largest muscle in the leg's anterior compartment-primarily enables foot dorsiflexion and inversion. Nearby, the extensor digitorum longus (EDL), a long muscle extending along the anterior leg, helps lift the foot and extend the toes. The trapezius, a large, superficial triangular muscle spanning the back and neck, contributes to head and shoulder movement.

In our study, we confirmed the expression of the RYR1 gene in the TA, EDL, and trapezius muscles of rabbits. Comparative analysis revealed that the trapezius muscle exhibited the highest levels of RYR1 expression, while the tibialis anterior showed the lowest. These findings were obtained using real-time PCR and further validated through agarose gel electrophoresis.

KEY WORDS

SERCA1; Tibialis anterior; Extensor digitorum longus; Soleus; Trapezius; Gastrocnemius muscle; Ventricle; Gene expression; RT-PCR

ARTICLE HISTORY

Received 03 November 2023; Revised 24 November 2023; Accepted 30 December 2023

Introduction

Ryanodine receptors (RyRs) are essential calcium release channels located within the junctional regions of the sarcoplasmic reticulum (SR), particularly in close proximity to the transverse (T) tubules or the muscle cell membrane [1]. These regions, often referred to as calcium release units (CRUs), serve as crucial sites where calcium ions are released into the cytoplasm during muscle activation. In skeletal muscle, the close alignment of RyRs with voltage-sensing calcium channels in the T-tubules allows for the efficient conversion of electrical signals into mechanical contraction.

Under electron microscopy, RyRs are identifiable as large, foot-like projections bridging the gap between the SR and the plasma membrane, contributing to their structural classification as part of a supramolecular complex. These channels play distinct roles in skeletal and cardiac muscle, yet they share structural similarities that help in understanding how variations in architecture relate to differences in function [2].

Structurally, RyRs are massive homotetrameric proteins exceeding 2 million Daltons in molecular weight. Three isoforms exist in mammals-RyR1, RyR2, and RyR3-each with distinct tissue distribution and physiological roles. RyR1 predominates in skeletal muscle, RyR2 in cardiac tissue, and RyR3 has more variable expression across tissues. The cytoplasmic region of the channel interacts with several regulatory proteins and is sensitive to modifications such as phosphorylation and oxidation. Meanwhile, the C-terminal region forms the actual pore through which calcium ions pass.

RyRs are modulated by a complex interplay of ions and proteins. Calcium, magnesium, ATP, and other small molecules regulate their opening and closing. Notably, magnesium can inhibit RyR activity by binding to specific sites on the channel that compete with activating calcium ions [3]. The dynamic balance between these ions determines whether the channel is active or inhibited. In addition, internal calcium within the SR can influence the channel from the luminal side, either through direct interaction with regulatory sites or by enhancing calcium "feedthrough" into the cytoplasm.

Intracellular calcium plays a central role in signal transduction, acting as both a charge carrier and a second messenger. In resting conditions, the concentration of free calcium in the cytoplasm remains very low compared to that in internal stores or the extracellular space. This steep gradient enables calcium to function effectively as a trigger for cellular events, such as muscle contraction, neurotransmitter release, and apoptosis. To prevent cytotoxicity, cells tightly regulate calcium movement using specialized channels, exchangers, and ATP-driven pumps.

In muscle cells, contraction is initiated when an action potential triggers the release of calcium from the SR through RyRs. In skeletal muscle, this occurs through a direct physical interaction between the dihydropyridine receptor (DHPR) in the T-tubules and RyR1 in the SR. In cardiac muscle, however, calcium-induced calcium release dominates, where an initial influx of calcium activates RyR2 to release more calcium from the SR. Relaxation follows as calcium is re-sequestered by SERCA pumps back into the SR [4].

Beyond muscle function, RyRs have significant roles in other systems such as the nervous system and bone. In neurons, they contribute to synaptic signaling, plasticity, and learning. In bone-resorbing osteoclasts, they help mediate intracellular calcium signaling essential for bone remodeling and secretion processes.
Our present focus is on understanding the expression and regulation of RyR1 in rabbit skeletal muscle, with particular emphasis on its physiological relevance in different muscle

***Correspondence:** Ms. Kiranbala Jena, Department of Biotechnology, Utkal University, Bhubaneswar, Odisha, India. email: kiranbalajena26@gmail.com

groups. This investigation aims to deepen insight into how RyR1 contributes to muscle performance and how its regulation may differ across various muscle types (Figure 1).

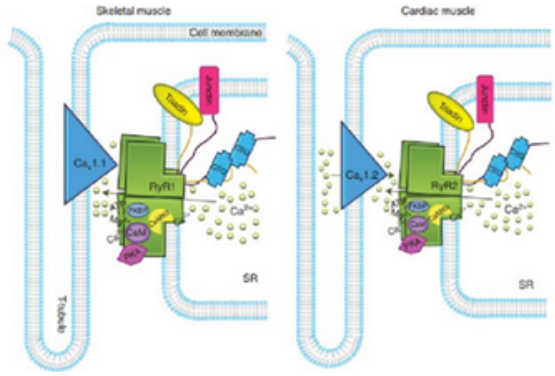

Figure 1. The interaction between RyR and various modulators.

The RYR1 gene encodes the ryanodine receptor type 1, a specialized calcium channel predominantly found in skeletal muscle tissue. This protein belongs to a broader family of ryanodine receptors that regulate the release of calcium ions from internal cellular stores, primarily the sarcoplasmic reticulum [5]. Upon activation, the RYR1 channel facilitates the rapid movement of calcium into the cytoplasm, a process that is essential for initiating muscle contraction and enabling voluntary movement (Figure 2).

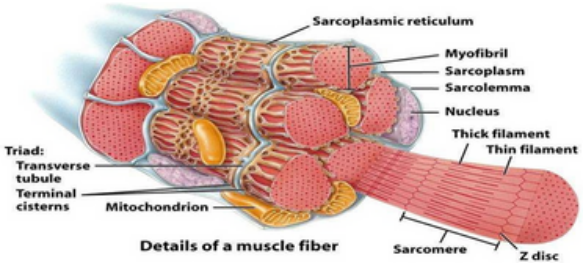

Figure 2. Details of muscle fiber structure.

Coordinated muscle movement depends on the precise contraction and relaxation of skeletal muscle fibers. These contractions are initiated by a rise in intracellular calcium levels. In resting muscle cells, calcium ions are sequestered within the sarcoplasmic reticulum, a specialized organelle that serves as a reservoir for calcium.

Ryanodine receptor type 1 (RyR1) channels are embedded in the membrane of the sarcoplasmic reticulum and function as regulated gateways for calcium release. When a muscle cell receives an electrical signal, RyR1 channels open to allow calcium ions to flow into the cytosol. This rapid increase in calcium concentration activates the contractile machinery of the muscle fiber, leading to contraction. This sequence of events, in which electrical stimulation leads to mechanical force generation, is known as excitation–contraction (E-C) coupling [6].

The RYR1 gene directs the synthesis of the RyR1 protein, a key regulator of calcium dynamics in skeletal muscle. Positioned along the membrane of the sarcoplasmic reticulum, RyR1 plays a vital role in controlling calcium release and, consequently, in enabling voluntary movement.

Muscle contraction is triggered by the rapid release of calcium ions (Ca^{2+}) from the sarcoplasmic reticulum (SR), initiated by depolarization of the transverse (T)-tubule membrane. Although the ryanodine receptor (RyR), which serves as the calcium release channel of the SR, has been successfully isolated and characterized, the precise mechanism by which T-tubule depolarization prompts calcium release remains incompletely understood. Two major hypotheses have been proposed: one suggests that calcium-induced calcium release (CICR) is the key mechanism, while the other supports a direct interaction between the voltage-sensing dihydropyridine receptor (DHPR) in the T-tubule and the RyR complex in the SR membrane.

Experimental recordings from single RyR channels reconstituted in artificial lipid bilayers have revealed their large conductance and sensitivity to various modulators. These channels are activated by micromolar levels of Ca^{2+} and millimolar concentrations of ATP, while inhibition is observed in the presence of millimolar Mg^{2+}, ruthenium red, and calmodulin [7]. Interestingly, ryanodine itself modifies the gating behavior of the channel, promoting prolonged open states interspersed with brief closures. This suggests that, within muscle cells, the RyR channel may be directly activated by Ca^{2+} and further regulated by intracellular factors such as ATP, Mg^{2+}, and calmodulin.

The gene encoding the ryanodine receptor from rabbit skeletal muscle has been cloned and expressed in mammalian cell lines, including Chinese hamster ovary (CHO) and COS-1 cells. Functional studies demonstrated that transformed CHO cells expressing RyR1 released calcium from intracellular stores in response to agents like caffeine and ryanodine, a property not observed in untransformed control cells. Similarly, RyRs expressed in COS-1 cells retained their responsiveness to physiological and pharmacological modulators, indicating that critical ligand-binding domains are intrinsic to the primary structure of the protein [8].

Comparative sequence analysis of ryanodine receptors has provided insights into their structural organization, including the identification of transmembrane regions and regulatory domains. A specific segment within the cardiac RyR, spanning amino acids 2619 to 3016, has been proposed as a modulator-binding region due to the presence of predicted binding motifs for ATP and calmodulin, along with phosphorylation sites. This domain, referred to here as "Modulator-Binding Region A," includes a calmodulin kinase-specific phosphorylation site at position 2809, which has been shown to enhance channel open probability. Interestingly, the corresponding site in the skeletal muscle RyR appears resistant to phosphorylation by calmodulin kinase, suggesting structural or regulatory divergence between cardiac and skeletal isoforms [9].

Beyond its well-established role in calcium-mediated muscle contraction, RYR1 also contributes significantly to the regulation of skeletal muscle development during embryogenesis. Its involvement in early myogenic signaling is supported by evidence linking RYR1-dependent calcium signaling to the expression of various genes critical for muscle formation. Notably, several of these genes belong to the Wnt signaling pathway, which plays a pivotal role in myogenic differentiation. In the absence of functional RYR1, developing muscle cells tend to form disorganized, underdeveloped clusters, indicating impaired morphogenesis. Furthermore, a reduction in RYR1 expression correlates with a shift in muscle fiber composition, particularly a marked decrease in type I (slow-twitch) fibers. These observations highlight a crucial, non-contractile function of RYR1 in orchestrating the molecular and structural maturation of skeletal muscle tissue during early development [10].

https://doi.org/10.61577/imb.2023.100005

Methods

Tissue

All experimental procedures involving rabbits were conducted in accordance with national ethical guidelines and approved animal care protocols. Animals were housed in controlled barrier facilities under standardized conditions. Euthanasia was performed humanely, either upon the onset of moribund condition or based on veterinary recommendation, without knowledge of treatment allocation. Following sacrifice, tissue samples were collected from multiple muscle groups, including the trapezius, extensor digitorum longus (EDL), soleus, tibialis anterior (TA), diaphragm, and ventricular muscle, for downstream analyses.

RNA extraction

Materials

- Rabbit muscle
- Trizol reagent
- Chloroform
- Isopropanol
- 70% Ethanol
- RNase free water

Homogenisation

For RNA extraction from rabbit muscle tissues, TRIzol reagent (Invitrogen Life Technologies) was utilized. This reagent, composed of phenol and guanidine isothiocyanate in a single-phase solution, is specifically designed for the efficient isolation of total RNA suitable for downstream applications such as PCR.

Muscle samples were placed in Eppendorf tubes along with stainless steel beads and an initial volume of TRIzol reagent. The tubes were then subjected to mechanical homogenization to ensure complete tissue disruption. Additional TRIzol was added in small increments during the process to enhance homogenization efficiency.

After homogenization, the samples were treated with chloroform and vigorously vortexed. The addition of chloroform-initiated phase separation, allowing for the selective isolation of RNA from other cellular components.

RNA isolation

The homogenized lysate was centrifuged at 12,000 × g to separate the aqueous phase. The resulting supernatant was carefully transferred to a fresh microcentrifuge tube, followed by the addition of pre-chilled isopropanol to precipitate the RNA. This mixture was then centrifuged again to facilitate RNA pellet formation.

Subsequently, the supernatant was removed, and the RNA pellet was washed with 70% ethanol. This ethanol wash step was repeated twice to ensure the removal of impurities and residual salts. Each wash was followed by centrifugation to retain the RNA pellet.

After the final wash, the supernatant was discarded, and the RNA pellet was air-dried to eliminate any remaining ethanol before downstream processing.

Qualitative and quantitative analysis

The dried RNA pellet was resuspended in RNase-free water and assessed for quality and concentration using agarose gel electrophoresis and NanoDrop spectrophotometry.

- **Agarose gel electrophoresis**: A 2% agarose gel was prepared with ethidium bromide incorporated for nucleic acid staining. Once the gel solidified, RNA samples were loaded into the wells. Electrophoresis was performed, and the gel was subsequently visualized under a UV transilluminator to assess the integrity and quality of the extracted RNA.
- **Nano drop spectrophotometry**: Quantification of RNA concentration was performed using a NanoDrop spectrophotometer, which allows measurement with minimal sample volume (approximately 2 µL). The RNA sample was placed directly onto the instrument's optical pedestal for analysis. Absorbance ratios at 260/280 and 260/230 were recorded to assess RNA purity.

cDNA synthesis

Materials

- PrimeScript RTase (200U/µL)
- 5XPrimeScript Buffer
- RNase Inhibitor(40U/µl)
- dNTP mixture
- Random 6 mer
- RNase free water

Synthesis

First-strand cDNA synthesis was carried out using the TaKaRa PrimeScript cDNA Synthesis Kit. This kit provides all essential components for reverse transcription from total RNA or polyadenylated RNA, utilizing PrimeScript RTase—an M-MLV-derived reverse transcriptase. The enzyme enables efficient synthesis of cDNA fragments up to 12 kb and performs optimally at 42°C, even when working with RNA templates containing high GC content or complex secondary structures. This eliminates the need for elevated temperatures that could compromise RNA integrity. The resulting first-strand cDNA is suitable for a range of downstream applications, including second-strand synthesis, PCR, real-time PCR, and hybridization techniques.

- **Step 1**: A reaction mixture containing random hexamer primers, dNTPs, RNase-free water, and template RNA was prepared in a microcentrifuge tube. The mixture was then incubated at 65°C for 5 minutes to denature the RNA. This thermal step is essential for disrupting secondary structures in the RNA, thereby enhancing the efficiency of the reverse transcription process.
- **Step 2**: The reverse transcription reaction was set up by combining the RNA-primer mixture from the previous step with 5X PrimeScript buffer, RNase inhibitor, PrimeScript RTase, and RNase-free water. The components were thoroughly mixed to ensure uniformity. The reaction mixture was then incubated under the following thermal conditions: 30°C for 10 minutes to facilitate primer annealing, followed by an extended incubation at 42–50°C for 30 to 60 minutes to allow for cDNA synthesis. To terminate the reaction and inactivate the enzyme, the mixture was heated to 95°C.

Real time polymerase chain reaction (RT-PCR)

Quantitative real-time polymerase chain reaction (qPCR), a molecular technique that enables real-time monitoring of DNA amplification, was employed to assess gene expression levels. Unlike conventional PCR, which measures amplified DNA at the end of the reaction, qPCR tracks the amplification process during each cycle.

https://doi.org/10.61577/imb.2023.100005

In this study, a nonspecific fluorescent dye-based detection method was utilized using Power SYBR™ Green (Applied Biosystems). The housekeeping gene 18S rRNA served as the internal control for normalization. The specific primer sequences used for amplification were:

- RYR1 Forward: CTACCTCCCACAGCATACTG
- RYR1 Reverse: TCATCAGCAGCTGCGAGGAG
- 18S rRNA Forward: AACAGATACGGTCGTACTTC
- 18S rRNA Reverse: TACCGTGAATTCCTATAAG

qPCR was carried out in CFX96 Real Time System thermo cycler by following these steps:

Initial denaturation and denaturation

At the start of the PCR protocol, an initial denaturation step was performed for 3 minutes to ensure complete separation of the DNA strands. This was followed by the first thermal cycling step, consisting of denaturation at 94°C for 15 seconds to maintain strand separation during amplification.

Annealing

Primers are short, single-stranded nucleic acid sequences, typically 20 to 30 bases long, that serve as initiation points for DNA synthesis. For the amplification of a specific target region, two primers are required: a forward primer and a reverse primer. During the annealing step of PCR, these primers hybridize to their complementary sites on the template DNA. This process was carried out at a temperature range of 47–60°C for 15 seconds to ensure proper binding and specificity.

Extension

Taq DNA polymerase, a thermostable enzyme obtained from the thermophilic bacterium Thermus aquaticus, was employed due to its ability to withstand high temperatures required for PCR. During the extension step, the reaction temperature was raised to 72°C for 30 seconds, allowing the enzyme to bind to the annealed primers and synthesize the complementary DNA strand. This process of denaturation, primer annealing, and extension was repeated for a total of 40 amplification cycles to ensure sufficient product yield.

Final hold

Upon completion of the 40 amplification cycles, the reaction temperature was reduced to 4°C, where the samples were held until further analysis.

Results

Quantitative estimation of RNA in sample through nano drop spectrophotometry

The RNA isolated from the muscle tissues was quantified using a NanoDrop spectrophotometer. The measured concentrations were as follows: tibialis anterior (TA) – 261.26 µg/µl, extensor digitorum longus (EDL) – 830.56 µg/µl, and trapezius – 1011.32 µg/µl (Figure 3-5).

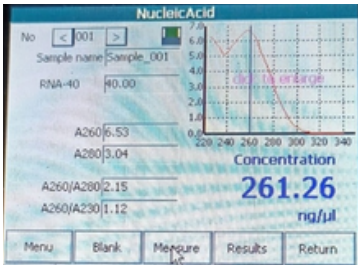

Figure 3. Nanodrop reading of TA.

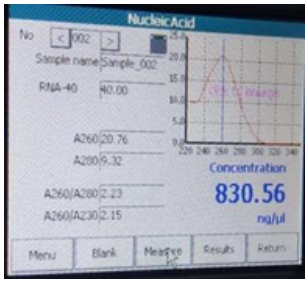

Figure 4. Nanodrop reading of EDL.

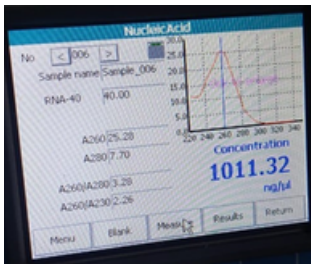

Figure 5. Nano drop reading of Trapezius

Visualization of RNA in agarose gel

The extracted RNA samples were loaded onto an agarose gel and subjected to electrophoresis. Distinct RNA bands were observed across all muscle tissues analyzed, with the trapezius muscle displaying the most prominent band intensity (Figure 6).

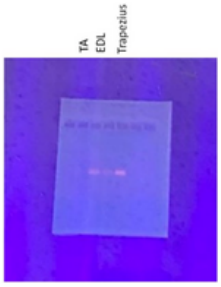

Figure 6. Visualization of RNA in TA, EDL and trapezius muscle.

Visualization of cDNA in agarose gel

To confirm successful cDNA synthesis, a portion of the reaction product was subjected to agarose gel electrophoresis alongside a 50 bp DNA ladder. When visualized under a UV transilluminator, a distinct band corresponding to cDNA was observed, indicating successful reverse transcription (Figure 7).

Figure 7. Agarose gel showing cDNA.

https://doi.org/10.61577/imb.2023.100005

Amplification and melt curves of 18srRNA reference gene and RYR gene in muscles

Following the completion of RT-PCR, both amplification and melt curves were analyzed. The expression levels of the RYR1 gene were evaluated in relation to the 18S rRNA reference gene across all three muscle types (Figure 8-10).

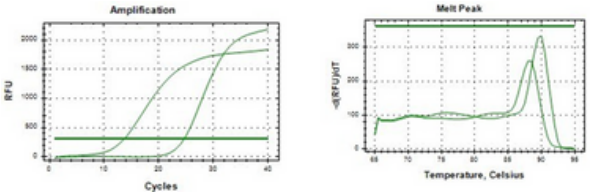

Figure 8. Amplification and melt curve of 18Srrna and RYR1 genes in TA muscle.

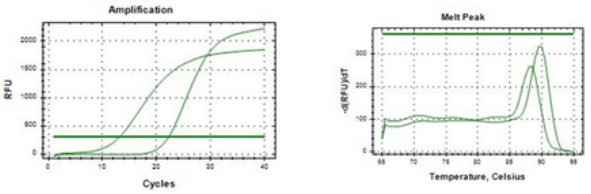

Figure 9. Amplification and melt curve of 18srRNA and RYR1 genes in EDL muscle.

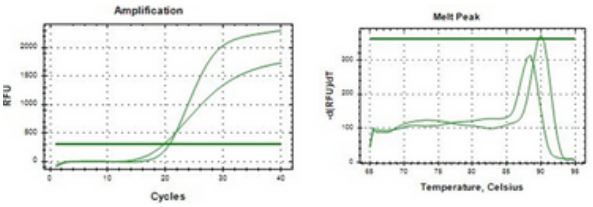

Figure 10. Amplification and melt curve of 18sr RNA and RYR1 gene in Trapezius muscle.

Amplification curve and melt curve showing comparison between TA, EDL and Trapezius muscles

Amplification and melting curves were plotted to compare RYR1 gene expression among the three muscles. The comparative profiles highlighted variations in Ct values and melting temperatures, indicating differential expression levels of RYR1 (Figure 11).

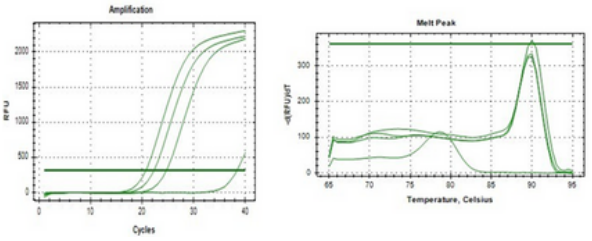

Figure 11. Amplification curve and melt curve showing comparison of RYR1 gene in TA, EDL and trapezius muscles of rabbit.

Amplification curve and melt curve showing comparison of 18srrna with RYR1 of TA, EDL and Trapezius muscle

Further analyses involved comparative amplification and melt curves of RYR1 and 18SrRNA genes across all three muscle types. These visualizations helped assess the relative gene expression of RYR1 normalized to the housekeeping gene (Figure 12).

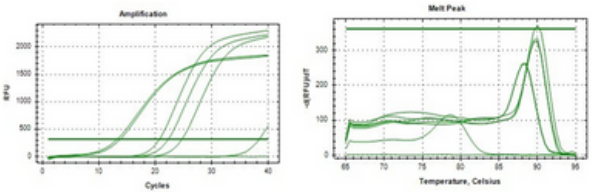

Figure 12. Amplification curve and melt Curve showing comparison of 18srRNA reference gene and RYR1 gene in TA, EDL and Trapezius muscles of rabbit.

Visualization of PCR product in agarose gel

Post-PCR amplification, the products were visualized on a 2% agarose gel alongside a 50 bp DNA ladder. Distinct bands corresponding to the expected size of the RYR1 gene fragment were observed for all three muscle types, confirming successful amplification (Figure 13).

Figure 13. Visualization of PCR product to verify amplification of cDNA.

Comparative analysis of RYR1 expression in TA, EDL and trapezius muscle

Quantitative analysis indicated the highest RYR1 gene expression in the Trapezius muscle, followed by moderate expression in EDL, and the lowest in the TA muscle. This pattern was consistent in both the gel electrophoresis results and real-time PCR data analysis (Figure 14).

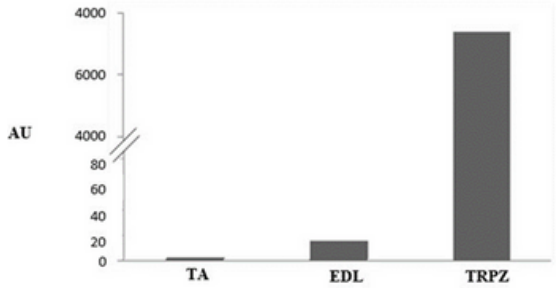

Figure 14. Comparative analysis of expression of RYR1 in TA, EDL and Trapezius.

https://doi.org/10.61577/imb.2023.100005

Discussion

Historically, the diagnosis and classification of RYR1-related disorders (RYR1-RD) have primarily relied on histopathological findings from muscle biopsies. However, the identification of new subtypes within the RYR1 disease spectrum has introduced complexity into the diagnostic process. As the field increasingly embraces a "genetics-first" approach to diagnosing inherited diseases, there is a growing need for standardized guidelines and consensus-driven frameworks to classify and name the diverse phenotypes associated with RYR1-RD [11]. The adoption of "RYR1-RD" as a unifying term represents an important initial step, though it may eventually be replaced by terminology that more comprehensively captures the heterogeneity of these disorders. A collective and timely discussion on this matter is both necessary and beneficial for advancing the understanding and management of this diverse group of neuromuscular conditions [12].

Conclusions

In this study, we examined the expression of the RYR1 gene in three distinct rabbit skeletal muscles: The Trapezius, Extensor Digitorum Longus (EDL), and Tibialis Anterior (TA). The findings demonstrated a clear pattern of differential gene expression among these muscle types. Notably, the Trapezius muscle exhibited the highest level of RYR1 expression, suggesting a greater involvement in calcium regulation and excitation–contraction coupling mechanisms. In contrast, the Tibialis Anterior showed the lowest expression levels, while the EDL presented with a moderate level of expression. These differences may reflect the functional and fiber-type composition of each muscle, contributing to their varied physiological roles. The results provide insights into the muscle-specific regulation of RYR1 and may have implications for understanding muscle function and the pathophysiology of RYR1-related disorders. Further research involving additional muscle types and functional assays could offer a more comprehensive understanding of RYR1 gene expression in skeletal muscles.

Disclosure Statement

No potential conflict of interest was reported by the author.

References

1. Santulli G, R Marks A. Essential roles of intracellular calcium release channels in muscle , brain, metabolism, and aging. Curr Mol Pharmacol. 2015;8(2):206-222. https://doi.org/10.2174/1874467208666150507105105
2. Meissner G. The structural basis of ryanodine receptor ion channel function. J Gen Physiol. 2017;149(12):1065-1089. https://doi.org/10.1085/jgp.201711878
3. Laver DR. Regulation of the RyR channel gating by Ca^{2+} and Mg^{2+}. Biophys Rev. 2018;10:1087-1095. https://doi.org/10.1007/s12551-018-0433-4
4. Peng W, Shen H, Wu J, Guo W, Pan X, Wang R, et al. Structural basis for the gating mechanism of the type 2 ryanodine receptor RyR2. Science. 2016;354(6310):aah5324. https://doi.org/10.1126/science.aah5324
5. Lawal TA, Todd JJ, Witherspoon JW, Bönnemann CG, Dowling JJ, Hamilton SL, et al. Ryanodine receptor 1-related disorders: an historical perspective and proposal for a unified nomenclature. Skelet Muscle. 2020;10:1-6. https://doi.org/10.1186/s13395-020-00243-4
6. Allard B. From excitation to intracellular Ca^{2+} movements in skeletal muscle: Basic aspects and related clinical disorders. Neuromuscul Disord. 2018;28(5):394-401. https://doi.org/10.1016/j.nmd.2018.03.004
7. Oo YW, Gomez-Hurtado N, Walweel K, van Helden DF, Imtiaz MS, Knollmann BC, et al. Essential role of calmodulin in RyR inhibition by dantrolene. Mol Pharmacol. 2015;88(1):57-63. https://doi.org/10.1124/mol.115.097691
8. Meissner G. The structural basis of ryanodine receptor ion channel function. J Gen Physiol. 2017;149(12):1065-1089. https://doi.org/10.1085/jgp.201711878
9. Marx SO, Marks AR. Dysfunctional ryanodine receptors in the heart: new insights into complex cardiovascular diseases. J Mol Cell Cardiol. 2013;58:225-231. https://doi.org/10.1016/j.yjmcc.2013.03.005
10. Tourel A, Reynaud-Dulaurier R, Brocard J, Fauré J, Marty I, Petiot A. RyR1 Is Involved in the Control of Myogenesis. Cells. 2025;14(3):158. https://doi.org/10.3390/cells14030158
11. Lawal TA, Todd JJ, Witherspoon JW, Bönnemann CG, Dowling JJ, Hamilton SL, Meilleur KG, Dirksen RT. Ryanodine receptor 1-related disorders: an historical perspective and proposal for a unified nomenclature. Skelet Muscle. 2020;10:1-6. https://doi.org/10.1186/s13395-020-00243-4
12. Lawal TA, Todd JJ, Meilleur KG. Ryanodine receptor 1-related myopathies: diagnostic and therapeutic approaches. Neurotherapeutics. 2018;15(4):885-899. https://doi.org/10.1007/s13311-018-00677-1

https://doi.org/10.61577/imb.2023.100005